Int. J. Heat Mass Transfer. Vol. 35, No. 2, pp. 567–581, 1992
Printed in Great Britain

0017–9310/92 $5.00+0.00

The structure of turbulence in rod bundles and the implications on natural mixing between the subchannels

KLAUS REHME

Kernforschungszentrum Karlsruhe GmbH, Institut für Neutronenphysik und Reaktortechnik, Postfach 3640, D-7500 Karlsruhe 1, F.R.G.

(*Received* 27 *August* 1990)

Abstract—The experimental data on natural mixing between subchannels of rod bundles by turbulent interchange are reviewed. The main features of the structure of turbulence in subchannels of rod bundles are discussed. It can be concluded that cyclic and almost periodic flow pulsations through the gaps of rod bundles are the reason for the observed mixing rates through the gaps which are relatively independent of the gap width. A simple correlation of a mixing factor is developed which may be used as a good approximation for any gap geometry.

INTRODUCTION

THE PREDICTION of the detailed temperature distribution of rod bundles, used especially as nuclear fuel elements, is required to ensure their safe and reliable operation. The rod-bundle thermal-hydraulic analysis is performed by solving the conservation equations for mass, momentum, and energy. The usual method for solving the conservation equations is by subchannel analysis since the methods of distributed parameter analysis are still under development. The subchannel analysis ignores the fine structures of velocity and temperature within the control volumes, the subchannels. Averaged mass flow rates and fluid temperatures are calculated within the individual control volumes. The turbulent interactions between the individual subchannels, which during the computation are assumed to act as independent parallel channels, are taken into account by mixing coefficients.

Following the nomenclature introduced by Todreas and co-workers [1, 2], we can distinguish between natural mixing effects and forced mixing effects. Forced mixing effects are caused by the presence of spacers or other geometrical disturbances. Natural mixing results from radial pressure gradients between adjacent subchannels, important in the entrance region where the inlet mass flow rate is redistributed among the subchannels or if the heat-flux distribution across a rod bundle is non-uniform. This kind of natural mixing is always directed from one subchannel into an adjacent one.

A non-directional effect of natural mixing results from natural eddy diffusion between the subchannels—turbulent interchange. Turbulent interchange causes an exchange of momentum, enthalpy or concentration between adjacent subchannels, however, without a net mass transport averaged in time. In this paper only the effects of turbulent interchange are discussed. First of all, the main contributions during the last three decades will be mentioned in which measurements of mixing coefficients have been reported and in which attempts have been made to interpret the interesting and sometimes surprising experimental results of mixing rate measurements.

REVIEW OF LITERATURE

Because of the importance of the mixing coefficients for the design of nuclear fuel elements the first review on mixing by Coates [3] appeared as early as 1960. This review was followed by those of Moyer [4] and Todreas and Wilson [1]. The early reviews mainly contained experimental data on forced mixing due to spacers. No attempts were made to correlate the few experimental natural mixing results available at that time or to explain their dependence on geometry.

The first important review was presented by Rogers and Todreas [2]. Based on the experimental data of Rowe and Angle [5], of Rapier [6], and of Rogers and Tarasuk [7], they stated the 'paradoxical relative independence of the mixing rate on the gap to diameter ratio'. They also mentioned that 'no information is available on the critical gap to diameter ratio below which the mixing rate decreases' and concluded that 'further experimental work is necessary especially on the structure of turbulence in large-scale models'.

Skinner *et al.* [8] were the first who attributed the higher rate of diffusivity in the gap to secondary flow since the mixing rates they measured were higher than could be accounted for by turbulent diffusion alone. Ingesson and Kjellström [9] replied that the results obtained by the secondary flow model of Skinner *et al.* could also be obtained by a turbulent diffusion model, however, with a much smaller effective mixing

NOMENCLATURE

A_i	cross-section of subchannel i [m^2]
B	band width [s^{-1}]
c_p	specific heat [J kg^{-1} K^{-1}]
D	rod diameter [m]
D_h	hydraulic diameter [m]
f	frequency [s^{-1}]
G	gap width [m]
K	constant [—]
L	length [m]
m_i	mass flow rate of subchannel i [kg s^{-1}]
P	pitch of rods [m]
P_i	wetted perimeter of subchannel i [m]
q_{ij}	heat transported between subchannels i and j per unit length [W m^{-1}]
R	radius of circular tube [m]
Re	Reynolds number [—]
S	gap width [m]
Str	Strouhal number [—]
T	subchannel bulk temperature [K]
u_{av}	average velocity in the axial direction [m s^{-1}]
u	axial velocity [m s^{-1}]
u'	fluctuating velocity in the axial direction [m s^{-1}]
u^*	friction velocity [m s^{-1}]
W	rod diameter plus gap between rod channel wall [m]
w'_{ij}	mixing rate between subchannels i and j [kg s^{-1} m^{-1}]
w'	fluctuating velocity in the direction parallel to the walls [m s^{-1}]
w_{eff}	effective mixing velocity [m s^{-1}]
w^M_{eff}	effective mixing velocity calculated by Möller [m s^{-1}]
$\hat{y}$	distance between the wall and the position of maximum velocity [m]
y^+	dimensionless distance from the wall [—]
Y	mixing factor [—]
z	coordinate along the wall [m]
z_{max}	distance from the gap between rod and channel wall to the symmetry line of the subchannel [m].

Greek symbols

β	mixing factor [—]
δ_{ij}	centroid distance between subchannels [m]
ε	eddy viscosity [m^2 s^{-1}]
$\bar{\varepsilon}$	reference eddy viscosity [m^2 s^{-1}]
ε_p	eddy viscosity parallel to the wall [m^2 s^{-1}]
ε_N	eddy viscosity normal to the wall [m^2 s^{-1}]
ε^+	non-dimensional eddy viscosity [—]
$\varepsilon^*_{\eta T}$	non-dimensional mixing coefficient [—]
λ_T	friction factor of the circular tube [—]
μ	molecular viscosity [kg m^{-1} s^{-1}]
$\mu_{M,T}$	mixing rate per unit length [m^{-1}]
ν	kinematic viscosity [m^2 s^{-1}]
ρ	density [kg m^{-3}]
Π	production of turbulent energy [m^2 s^{-3}]
τ_w	wall shear stress [N m^{-2}]
τ_p	shear stress parallel to the wall [N m^{-2}]
Φ	power spectral density per band width [m^2 s^{-1}].

Subscripts

i	subchannel i
j	subchannel j.

length than the distance between the centres of the subchannels.

In 1970, Ingesson and Hedberg [10] published a correlation of a mixing factor taking into account all relevant experimental results at that time. Their mixing factor is a multiplier on a reference eddy diffusivity which was assumed to be a characteristic value of the eddy diffusivity in circular tubes. Ingesson and Hedberg mentioned that the differences between experimental mixing factors of rod bundles arranged in triangular and in square arrays are not as large as some of the published correlations indicate.

An important observation was reported in 1970 by van der Ros and Bogaardt [11]: "visual observation and fast thermocouples indicate that the transport through the gap cannot be explained by eddy diffusivity. The thermocouple recordings as well as the visible waves are very regular in amplitude and frequency in the gap". This is the first time that indications of a large-scale structure through the gaps have been reported although Hofmann [12] in 1964 had visualized such structures in a seven-rod bundle using aluminium particles but never published his extremely interesting results. The experimental results by Galbraith and Knudsen [13] were a significant contribution to the data base on mixing rates. Especially their results in a square array with a pitch-to-diameter ratio of as low as $P/D = 1.011$ showed surprisingly high mixing rates. Also the data by Singh and St. Pierre [14] showed that the mixing rate increases with decreasing gap width in the range of $P/D = 1.102$–1.02 for a square array and a fixed Reynolds number of $Re = 2 \times 10^4$. Again, this effect was explained by secondary flows following the ideas of Skinner *et al.* Eifler and Nijsing [15] showed theoretically using the modelling they developed in 1971 that the greater part of the mixing rate was caused by secondary flow rather than by turbulent diffusion. Due to their model, for $P/D = 1.1$, the contribution to the mixing rate by turbulent diffusion is only one-tenth of the total mix-

ing rate for the momentum transport between a triangular and a square subchannel. With higher pitch-to-diameter ratios the contribution of the turbulent diffusion increases to about one-third at $P/D = 1.7$.

In 1972, Rowe *et al.* [16, 17] published his laser-Doppler measurements in rod bundles arranged in a square array. His results significantly show that there exists an additional macroscopic flow process in the regions adjacent to the gaps, i.e. large scale turbulence moves through the gaps which can be considered as a periodic flow pulsation across the gaps. Moreover, Rowe found dominant turbulence frequencies for a considerable distance along the centreline traverses for the narrower gap spacings and both in the interior and in the wall and corner subchannels. Rowe also discussed the implications of the large-scale turbulent motion on the mixing between adjacent subchannels. He concluded that the flow pulsations explain the weak influence of rod gap spacing on rod bundle intersubchannel mixing. Another important conclusion by Rowe is that the shape of subchannels adjacent to a rod gap does not significantly affect the turbulence parameter distribution in the gap.

In the light of Rowe's results, Rogers and Tahir [18] mentioned the macroscopic flow pulsations as an additional effect to enhance the mixing through the gaps of rod bundles. However, they believed that secondary flow plays an important role to explain the weak dependence of the mixing rates on the gap to diameter ratio although no convincing experimental results had been reported on secondary flow in rod bundles. Moreover, Rogers and Tahir felt that both secondary flow and the additional large-scale periodic eddies reduce the mixing distance as the gap to diameter ratio decreases.

Seale [19] concluded from his investigations of heat transfer across a rod bundle that anisotropic diffusivities are the reason for the high mixing in narrow gaps of rod bundles. He also found the mixing coefficients predicted by Ingesson and Hedberg [10] to be high by a factor of two. This was also mentioned earlier by Kjellström [20], Markoczy and Huggenberger [21], Martelli [22] and Cevolani [23].

The macroscopic flow pulsations observed by Rowe [16] have been confirmed and stressed by Hooper and Rehme [24, 25] by hot-wire measurements in a four-rod bundle. Their results show that there exists an energetic and almost periodic azimuthal turbulent-velocity component directed through the gap. The azimuthal turbulent-velocity component is not associated with mean secondary-flow velocities driven by Reynolds-stress gradients.

More recent reviews on mixing were published by Cheng and Todreas [26, 27] and Zhukov *et al.* [28]. Both reviews concentrate on rod bundles spaced by wire-wraps but they also report correlations for the mixing rate in bare rod bundles. Whereas Cheng and Todreas do not comment on the reasons for the high mixing rates at low gap to diameter ratios, Zhukov *et al.* explain the mixing rates by secondary flow effects.

STRUCTURE OF TURBULENCE IN ROD BUNDLES

First, we will discuss our present knowledge on the structure of turbulence in rod bundles. As mentioned before, Rogers and Todreas [2] concluded in 1968 that a detailed knowledge on the structure of turbulence is necessary to understand how the mixing rates depend on the gap to diameter ratio.

Secondary flow

Most attempts to measure Reynolds stress driven secondary flows in rod bundles were not successful, e.g. by Hall and Svenningson [29], Trupp and Azad [30] and Carajilescov and Todreas [31], either due to geometrical tolerances of the test sections which caused cross flow or due to experimental inaccuracy. Secondary flows have been shown to exist in non-circular channels by Nikuradse [32] for different channel geometries. Reliable experimental data on secondary flows have been reported by Hoagland [33], Brundrett and Baines [34], Gessner and Jones [35], Launder and Ying [36] and Melling and Whitelaw [37] for square and rectangular ducts, by Aly *et al.* [38] for a triangular duct, and by Khalifa and Trupp [39] for a trapezoidal duct. The unique feature of all ducts for which experimental data have been obtained is that these ducts have corners in their shapes.

Therefore, it is not surprising that Seale [40] measured secondary flows in his duct of a simulated rod bundle which also had corners. Effects of secondary flow in a corner subchannel of a square array have also been found in refs. [41, 42], especially deduced from the contours of the kinetic energy of turbulence which in the corner of the bundle were very similar to those found in the corner of a square duct. Seale [43, 44] however, from his experimental and numerical investigations in a parallel subchannel duct, concluded that secondary flows are insignificant for the high mixing rates (gap Stanton numbers) observed experimentally. He showed that only predictions by using highly anisotropic eddy viscosities could satisfactorily represent his experimental data.

Vonka [45] reported experimental data on secondary flows in a central subchannel of a triangular array. He found that the magnitude of the secondary flow velocity is less than 0.1% of the axial velocity. In reality, Vonka measured cross flow velocities of the order of 1% of the axial velocity which were caused by cross flow from the inner subchannels into the outer ones due to not fully developed flow and also due to the blockage of the outer subchannels by the spacers. This blockage causes a cross flow into the inner subchannels at the spacer level which downstream of the spacer redistributes. Vonka extracted the secondary flow velocities of less than 0.1% of the axial flow velocity from the measured cross flow velocities of 1% of the axial velocity.

Neelen [46] analysed many experimental data on turbulence and velocity distributions in rod bundles

and concluded that secondary flows in rod bundles are very small and can be neglected. Neelen found, in agreement with Monir [47], that if the eddy viscosities parallel to the walls are modelled in agreement with the experimental results in rod bundles, modelling of secondary flows does not improve the agreement between predictions and experimental results on distributions of wall shear stresses and velocity. These findings confirmed the observations by Seale [43, 44], Bartzis and Todreas [48], and Rehme [42, 49].

The conclusion from the above discussions on secondary flows in rod bundles is that the secondary flow velocities are very small. It is obvious that secondary flows do not contribute significantly to the mixing between subchannels of rod bundles since the secondary flow vortices are expected to move within the elementary cells of the subchannels. They do not cross the gaps between the subchannels. Therefore, secondary flows cannot be the reason for the high mixing rates measured for low gap-to-diameter ratios as was assumed in the past.

Reynolds stresses

Systematic and detailed experimental investigations of the Reynolds stresses have been performed at the Karlsruhe Nuclear Research Centre since 1974 [49]. Hot-wires have been used for the measurements in 17 different geometries of four rods arranged parallel in a rectangular channel. The pitch-to-diameter ratios covered the range between 1.036 and 1.40, the wall-to-diameter ratios the range between 1.026 and 1.40. Most references of the data reports are given in ref. [50], the results from some additional geometries are reported in refs. [51–53].

Only the most striking features which were observed in rod bundles will be discussed. These are features which show the strongest differences between turbulent flow through rod bundles and through simple channels like circular tubes and parallel plates. A typical experimental result of the axial turbulence intensity is shown in Fig. 1 measured in a geometry with a pitch-to-diameter ratio (P/D) of 1.148 and a wall-to-diameter ratio (W/D) of 1.045 at $Re = 6.11 \times 10^4$. The contours of the axial turbulent intensity are scaled by the wall friction velocity in the gap between the rods. The contour plot was produced by a computer program without any smoothing of data. The measurements in the four quadrants and in the parts of the quadrants divided by the line of maximum normal distance from the walls were performed at different times. One plot was produced of the result in each part of the quadrants. The plots were then joined, with the result that small steps occur on the contours at the line of maximum normal distance from the walls. The tick marks indicate the traverses on which data have been measured, in circular coordinates close to the rod walls and in Cartesian coordinates close to the channel walls, respectively.

The contours of the axial turbulence intensity are almost symmetrical for a ratio of length-to-hydraulic diameter $L/D_h = 146.3$. Small asymmetries stem from the conditions at the entrance of the test section [54]. In the region around the gap between the rods, the axial intensities are high at the walls and drop toward the lines of maximum normal distance from the walls. It is interesting to note that there are regions of relatively high axial turbulence intensity on the lines of maximum normal distance from the walls. These saddle points are located on both sides at about 25° from the gap between the rods. The observations are quite different in the regions around the gaps between the rods and the channel walls. These gaps are narrower than the gap between the rods. The highest axial turbulence intensities in the cross-section are found on the lines of maximum normal distance from the walls at about 35° from the gap between the rods and channel walls. The axial turbulence intensities are higher than the highest intensities at the walls. Therefore, these high axial turbulence intensities have not been produced by wall turbulence and transported by secondary flows. The maximum value of the axial turbulence intensity depends on the relative gap width, i.e. P/D or W/D, respectively. The maximum value increases with decreasing gap width as was shown in ref. [55].

Another example which is typical for the structure of turbulence in rod bundles is shown in Fig. 2. It displays the turbulence intensities parallel to the wall measured along the line of normal distance from the walls vs the non-dimensional distance along the channel wall. The turbulence intensities parallel to the wall are normalized by the local friction velocity along the channel wall. The coordinate z along the wall is zero in the gap between the rod and channel wall and has the value z_{max} at the symmetry line normal to the channel wall (refer to Fig. 1). The data are shown for eight different wall-to-diameter ratios. The striking feature is that the intensity parallel to the walls on the line of maximum distance increases systematically with decreasing wall-to-diameter ratio, i.e. decreasing relative gap width between the rod and channel walls. The maximum values are found for $z/z_{max} = 0$, that is, directly in the gap between the rod and channel wall. The data for the centre of circular tubes established by Lawn [56] is indicated in Fig. 2. For $W/D < 1.148$, the intensity parallel to the wall on the line of maximum normal distance from the walls is higher than in the centre of circular tubes. As has been discussed in ref. [55], the intensity parallel to the walls is even higher than the axial turbulence intensity directly in the gap between the rod and the channel wall for $W/D \leqslant 1.048$.

The eddy viscosity parallel to the wall can be calculated from the measured shear stress parallel to the wall $\tau_p = -\rho\overline{u'w'}$ and the velocity gradient parallel to the wall as

$$\varepsilon_p = \frac{-\overline{u'w'}}{\partial u/\partial z}. \tag{1}$$

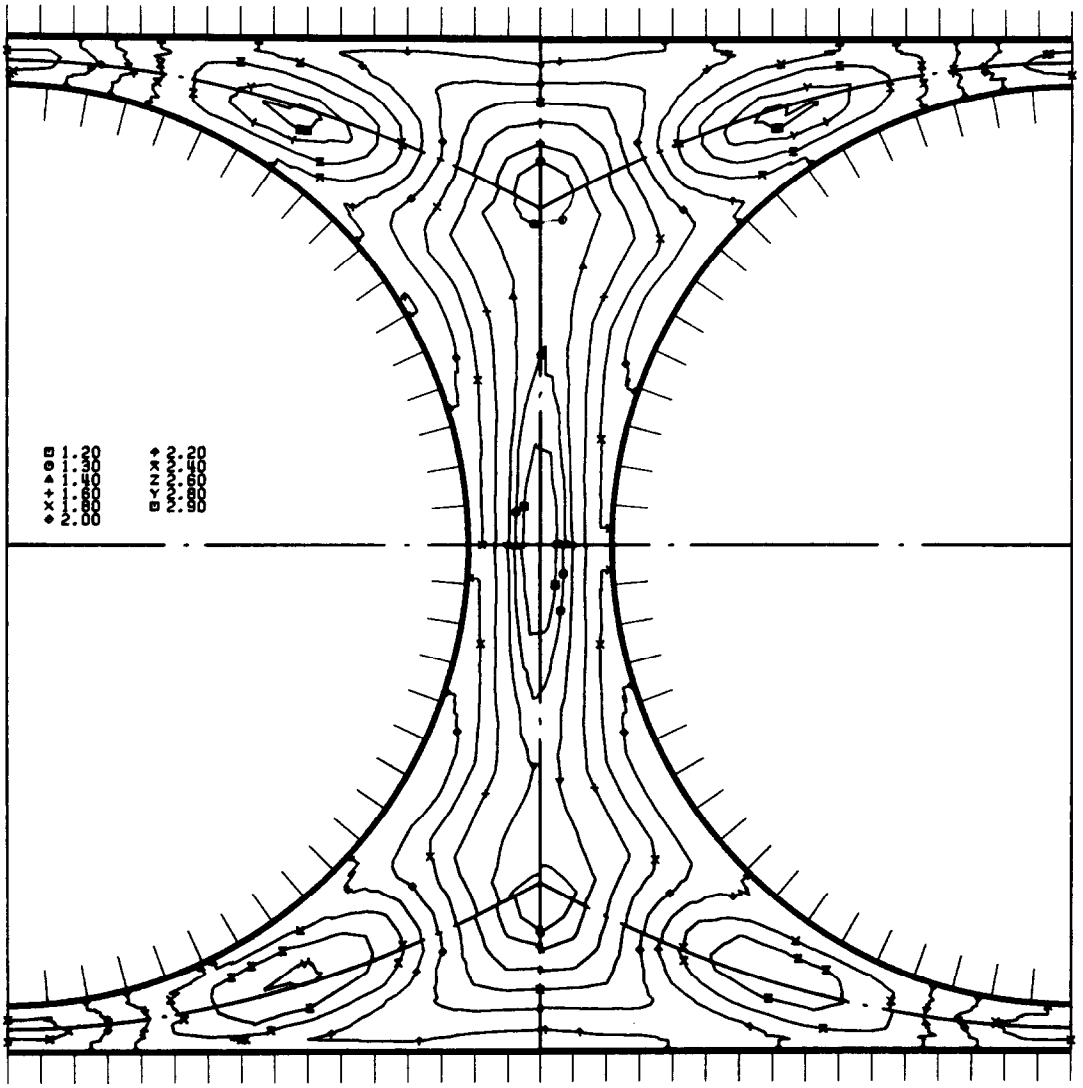

FIG. 1. Contours of axial turbulence intensity in a rod bundle of $P/D = 1.148$, $W/D = 1.045$, $L/D_h = 146.3$ and $Re = 6.11 \times 10^4$.

The dimensionless eddy viscosity parallel to the wall

$$\varepsilon_p^+ = \frac{\varepsilon_p}{u^* \hat{y}} \tag{2}$$

is related to the local friction velocity

$$u^* = \sqrt{\left(\frac{\tau_w}{\rho}\right)} \tag{3}$$

and the length of the velocity profile between the wall and the line of maximum normal distance from the walls $\hat{y}$.

Figure 3 displays all data measured in the test sections mentioned above [50–53] together with the only other available data which presents eddy diffusivities parallel to the walls as a function of the relative gap width S/D, which is by Tahir and Rogers [57] and by Hejna and co-workers [58, 59]. The data shown were measured close to the gaps since directly in the gap the velocity gradient parallel to the walls vanishes and the eddy viscosities parallel to the walls are undefined. There is a considerable scatter of the data which is mainly due to the calculation of the velocity gradient and slight asymmetries in the velocity distribution because of fabrication tolerances of the test sections and entrance effects. However, it is obvious that the eddy viscosities parallel to the walls strongly increase with decreasing relative gap width. A least square fit of the data in the log–log plot yields

$$\varepsilon_p^+ = 0.0177\left(\frac{S}{D}\right)^{-2.42} \tag{4}$$

which shows the strong dependence on the relative

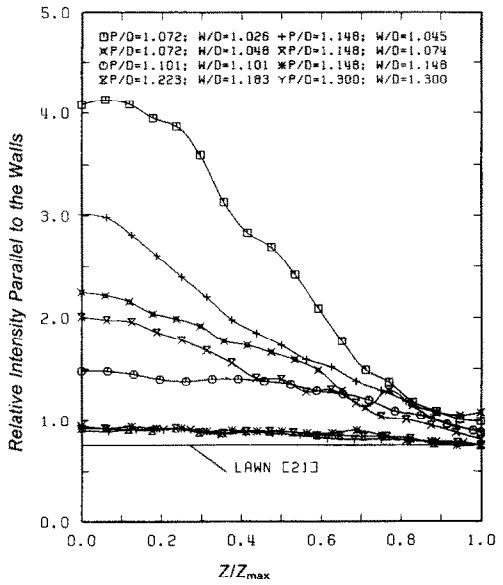

FIG. 2. Relative turbulence intensity parallel to the channel wall along the line of maximum normal distance from the rod and channel wall vs non-dimensional distance along the channel wall.

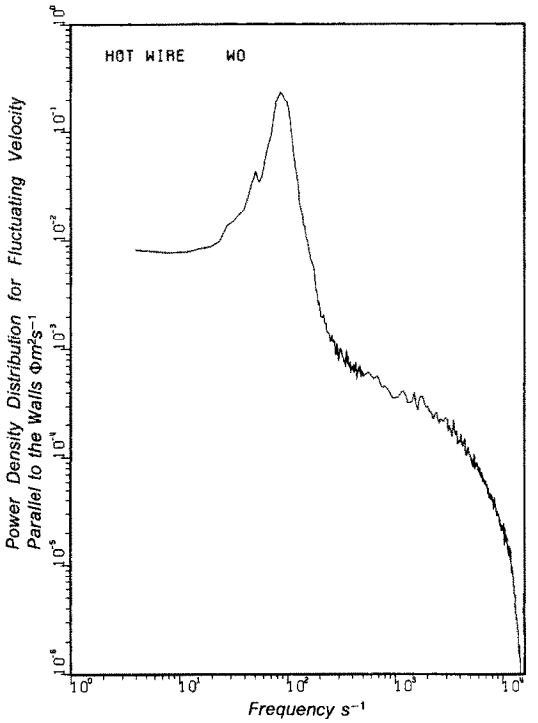

FIG. 4. Power spectral density of the velocity parallel to the wall in the centre of the gap between the rods for a rod bundle of $P/D = 1.036$ and $W/D = 1.072$.

gap width. It is interesting to note that a least square fit of either the data for the rod–rod gap or the rod–wall gap gives almost the same results as equation (4).

The experimental eddy viscosities normal to the wall are nearly independent of the relative gap width and are comparable to the data of circular tubes by Reichardt [60] close to the walls [50, 57, 58]. The eddy viscosities normal to the wall are slightly higher (up to a factor of two) than at the centre of circular tubes in the region close to the maximum normal distance from the walls [50, 57, 58]. The comparison between the eddy viscosities parallel to the walls in rod bundles (Fig. 3) and the eddy viscosity normal to the wall at the centre of circular tubes [60]

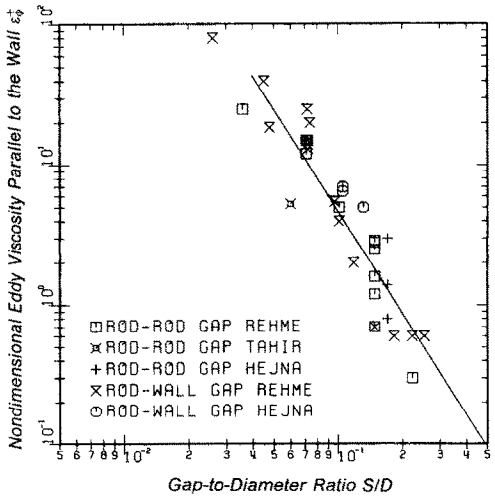

FIG. 3. Eddy viscosity parallel to the wall close to the gaps in rod bundles vs the gap-to-diameter ratio.

$$\varepsilon_N^+ = \frac{\varepsilon_N}{u^* R} = 0.066 \qquad (5)$$

shows that the anisotropy of the eddy viscosities strongly increases with decreasing gap width for turbulent flow through rod bundles.

Macroscopic flow pulsations

The macroscopic flow pulsations in rod bundles which were first observed by Hofmann [12], by van der Ros and Bogaardt [11] and by Rowe [16] have been confirmed by Hooper and Rehme [25]. Recently, Möller [61, 62] investigated the macroscopic flow pulsations systematically in different rod bundle geometries (P/D, W/D). Möller found peaks at characteristic frequencies in the power spectra of the turbulent velocity fluctuations in the axial direction (u') and the direction parallel to the walls (w'). A typical example is shown in Fig. 4 for the w'-component in the gap between the rods for a $P/D = 1.036$ [58]. The characteristic frequency f, first mentioned by Rowe [16], varies with the gap geometry (P/D or W/D, respectively). The frequency f increases with decreasing gap width at the same Reynolds number based on the mean subchannel velocity and the hydraulic diameter of the subchannel. The frequency varies linearly with the Reynolds number which was already found by Hooper and Rehme [25]. Möller showed that a Strouhal number, defined with the characteristic frequency f, the rod diameter D, and

the friction velocity u^* in the gap between the rods or between the rod and channel walls

$$Str = \frac{fD}{u^*} \tag{6}$$

only depends on the relative gap width S/D. The relative gap width is

$$S/D = P/D - 1 \tag{7}$$

in the case of the gap between the rods and

$$S/D = W/D - 1 \tag{8}$$

in the case of the gap between the rods and channel walls. Möller also found that the Strouhal number is independent of the type of gap (rod–rod or rod–wall) considered.

The peaks in the power spectra are highest for the fluctuating velocity component w' parallel to the wall directly in the gaps. With decreasing gap width, the peak becomes narrower in the frequency range and reaches a higher maximum value. The latter means that the average velocity through the gap increases with decreasing gap width. For higher gap width the peak broadens and the maximum value decreases. The broadening of the peak means that large eddies of different scales are responsible for the flow pulsations between subchannels. Möller [61] found that strong flow pulsations through the gap exist through a gap between the rods for a pitch-to-diameter ratio as low as $P/D = 1.007$. For this investigation the centre of the gap had a dimensionless distance from the wall of $y^+ = 22.4$.

The large-scale eddies move almost periodically through the gaps of rod bundles at the characteristic frequency. These macroscopic flow pulsations by the large-scale eddies cover almost the full cross-section of the subchannel as cross-correlation measurements have shown [25, 61]. The large-scale eddies through the gap between the rods move from the region of largest extent of one subchannel through the gap to the region of largest extent in the adjacent subchannel. The corresponding large-scale eddies through the gap between rod and channel wall move from the symmetry line of one subchannel (z_{max}) through the gap to the symmetry line of the adjacent subchannel.

The source of the turbulent energy which drives the large-scale eddies is the product of the shear stress parallel to the walls times the velocity gradient parallel to the walls

$$\Pi = \overline{u'w'}\frac{\partial u}{\partial z}. \tag{9}$$

The measurements of the structure of turbulence have shown that both $\overline{u'w'}$ and $\partial u/\partial z$ are of considerable magnitude on the line of maximum distance from the walls in the middle of the region between the gaps and the largest extent of the cross-section of the subchannels.

The existence of the large-scale eddy motion was confirmed by cross-correlation measurements of the temperature fluctuations by Horanyi *et al.* [63].

The periodic flow pulsations across the gaps in rod bundles are the true reason for the high mixing rates between subchannels in rod bundles. Both the increasing maximum values of the power spectra and the increasing characteristic frequency with decreasing gap width result in the well-known fact that the mixing rates are almost independent of the relative gap width.

NATURAL MIXING IN ROD BUNDLES

Definition

The fluctuating transverse mass flow rate per unit length w'_{ij}, called the mixing rate, between two subchannels through the gap S is defined as

$$w'_{ij} = \rho w_{eff} S \tag{10}$$

where w_{eff} is the effective mean mixing velocity. It should be noted that the time mean value of the fluctuating transverse mass flow rate is zero. Therefore, no net mass exchange results.

The heat transported through the gap per unit length by the effective mixing velocity is

$$q_{ij} = \rho c_p w_{eff} S(T_i - T_j) \tag{11}$$

where T_i and T_j are the bulk temperatures of subchannels i and j.

The experimental data on mixing rates and the correlations of mixing rates are reported in the literature by using different dimensional or non-dimensional parameters. For details of the experimental techniques see ref. [64]. To compare the different results, the method of a mixing factor introduced by Ingesson and Hedberg [10] is adopted in the following. Ingesson and Hedberg defined the heat transported through the gap per unit length by

$$q_{ij} = \rho c_p \bar{\varepsilon} S Y \frac{T_i - T_j}{\delta_{ij}} \tag{12}$$

where δ_{ij} is the mixing distance which is assumed to be the centroid distance between the subchannels i and j and $\bar{\varepsilon}$ is a reference eddy viscosity. The mixing factor Y is a multiplier which takes into account how much higher the effective eddy viscosity is in comparison to the reference eddy viscosity. At the same time, it includes the corrections for the approximation of the temperature gradient in the gap by the bulk temperature difference between the subchannels divided by the centroid distance. It is convenient to use the centroid distance δ_{ij} because this distance is exactly defined for all geometries and the bulk temperatures are computed in the subchannel codes.

The reference eddy viscosity is assumed to be

$$\bar{\varepsilon}^+ = 0.1 \tag{13}$$

which is often referred to as the dimensionless eddy viscosity at the centre of a circular tube. However, as

mentioned before, the dimensionless eddy viscosity at the centre of a tube is $\varepsilon^+ = 0.066$ [60].

With

$$\varepsilon^+ = \frac{\varepsilon}{Ru^*} \tag{14}$$

and

$$u^* = u_{av}\sqrt{\left(\frac{\lambda_T}{8}\right)} \tag{15}$$

the reference eddy viscosity can be expressed by

$$\bar{\varepsilon} = \frac{\nu}{20} Re\sqrt{\left(\frac{\lambda_T}{8}\right)} \tag{16}$$

which was already used by Moyer [4] and Rapier [6].

A comparison between equations (11) and (12) yields

$$Y = \frac{w_{eff}\delta_{ij}}{\bar{\varepsilon}}. \tag{17}$$

Experimental data

All relevant data in rod bundles have been re-evaluated in terms of the mixing factor Y. Most of the data cited by Ingesson and Hedberg have been used, however, corrected by a factor 1.14 to

$$Y = \frac{Y_{Ingesson}}{1.14} \tag{18}$$

because Ingesson and Hedberg used a value of $\varepsilon^+ = 0.0877$ as the reference viscosity based on the measurements of Elder [65]. The equations to recalculate reported mixing rates or gap Stanton numbers are given in the Appendix. To have a common basis, all mixing factors in Table 1 are given for $Re = 5 \times 10^4$. The data by Ingesson and Hedberg include the data reported by Bell and LeTourneau [66], Biggs and Rust [67], Bishop *et al.* [68], Clarke [69], Collins and France [70], Ingesson *et al.* [71], Jonsson [72, 73], Knaab and Stehle [74], Multer [75], Nelson *et al.* [76], Rowe and Angle [5], Rogers and Tarasuk [77] and Waters [78].

The gap Stanton numbers reported by Cheng and Todreas [26] were recalculated in terms of the mixing factor. The data include those of Petrunik [79], Kjellström [80], Roidt *et al.* [81], Rogers and Tahir [18], Walton [82], Kelly and Todreas [83] and Singh and St. Pierre [14]. All mentioned data are plotted in Fig. 5 together with the data by Galbraith and Knudsen [13], Castellana *et al.* [84], Seale [19] and Zhukov *et al.* [85].

No attempt was made to distinguish between the different subchannel sizes since there is more than one indication in the literature that the subchannel geometry is not very important for the mixing factor [10, 16, 17]. The scatter of the data is considerable. However, the scatter is not surprising due to geometrical tolerances of the test sections, the measuring techniques, and the disturbances of the flow fields by the probes and by spacers. Moreover, very long L/D_h ratios are required to reach fully developed flow without cross flows caused by pressure differences between the subchannels [54].

Table 1. Experimental mixing factors

Gap ratio S/D	Mixing factor Y	Source
0.20	8.19	Ingesson: Bishop *et al.*
0.11	16.7	Ingesson: Collis and France
0.033	27.0	Cheng: Petrunik
0.068	5.18	Cheng: Petrunik
0.13	2.83	Cheng: Petrunik
0.217	1.35	Cheng: Kjellström
0.256	1.49	Cheng: Roidt *et al.*
0.4	0.82	Cheng: Rogers and Tahir
0.068	4.8	Cheng: Walton
0.10	3.4	Cheng: Kelly and Todreas
0.15	3.31	Zhukov
0.214	1.48	Zhukov
0.32	0.35	Zhukov
0.13	1.84	Zhukov
0.011	109.0	Galbraith and Knudsen
0.028	28.9	Galbraith and Knudsen
0.063	11.3	Galbraith and Knudsen
0.127	8.38	Galbraith and Knudsen
0.228	5.5	Galbraith and Knudsen
0.334	3.36	Castellana *et al.*
0.13	8.16	Ingesson: Bell and LeTourneau
0.20	5.99	Ingesson: Bell and LeTourneau
0.40	1.90	Ingesson: Biggs and Rust
0.26	4.75	Ingesson: Nelson *et al.*
0.018	23.2	Cheng: Singh and St. Pierre
0.043	16.6	Cheng: Singh and St. Pierre
0.102	7.06	Cheng: Singh and St. Pierre
0.10	6.14	Seale
0.375	1.90	Seale
0.83	0.67	Seale
0.10	24.8	Ingesson: Clarke
0.62	2.03	Ingesson
0.10	11.6	Ingesson
0.16	3.64	Ingesson: Jonsson
0.14	7.84	Ingesson: Jonsson
0.19	5.34	Ingesson: Knaab and Stehle
0.20	9.82	Ingesson: Multer
0.15	4.39	Ingesson: Rowe and Angle
0.03	18.1	Ingesson: Rowe and Angle
0.08	19.4	Ingesson: Tarasuk and Kempe
0.20	6.77	Ingesson: Waters

A least square fit of all data yields

$$Y = \frac{0.7}{S/D}. \tag{19}$$

CORRELATIONS

To compare equation (19) with some correlations reported in the literature, the following correlations were chosen and recalculated as Y-factors by the equations given in the Appendix:

(a) Ingesson and Hedberg [10]

$$Y = K\left(\frac{P/D}{P/D-1}\right)^{1/2}\left(\frac{P}{D}\frac{P}{D_h}\right)^{3/2} \tag{20}$$

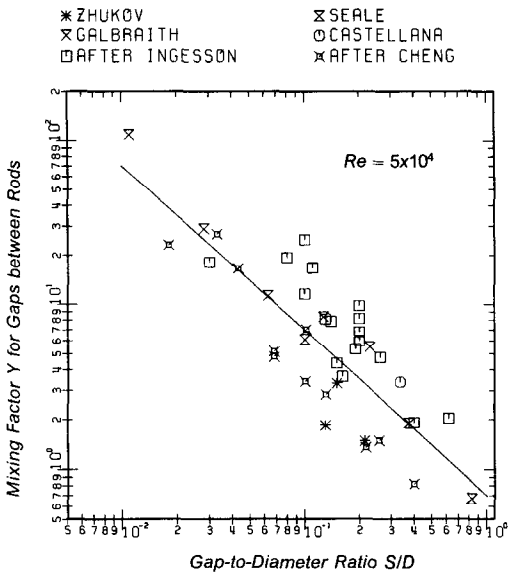

FIG. 5. Experimental mixing factors Y for gaps between the rods vs the gap-to-diameter ratio.

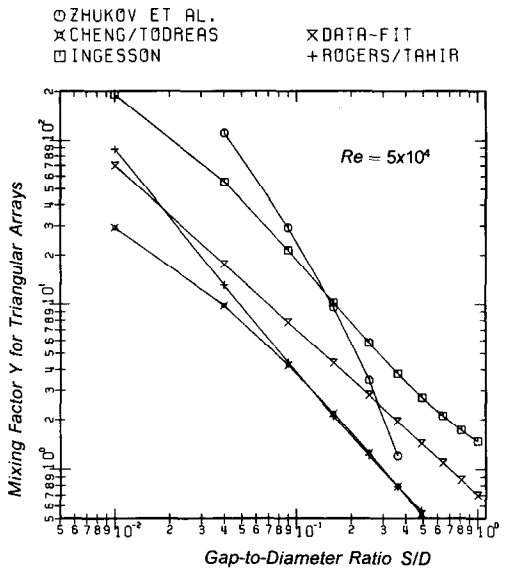

FIG. 6. Correlations for the mixing factor Y of rod bundles arranged in a triangular array.

where $K = 1.158$ and 0.933 for square arrays and triangular arrays, respectively.

(b) Rogers and Tahir [18]

$$\frac{w'_{ij}}{\mu} = 0.0018\, Re^{0.9}\left(\frac{S}{D}\right)^{-0.4} \quad \text{for triangular arrays} \tag{21}$$

$$\frac{w'_{ij}}{\mu} = 0.0050\, Re^{0.9}\left(\frac{S}{D}\right)^{0.106} \quad \text{for square arrays.} \tag{22}$$

(c) Cheng and Todreas [26]

$$\varepsilon^*_{\eta T} = 0.0016\left(\frac{S}{D}\right)^{-0.5} \quad \text{for triangular arrays} \tag{23}$$

$$\varepsilon^*_{\eta T} = 0.0056\left(\frac{S}{D}\right)^{-0.3} \quad \text{for square arrays.} \tag{24}$$

(d) Zhukov *et al.* [28]

$$\mu_{M,T} = \frac{0.0293 - 0.051(P/D - 1)}{\left|\frac{2\sqrt{3}}{\pi}\left(\frac{P}{D}\right)^2 - 1\right| Re^{0.1}\, D} \quad \text{for triangular arrays.} \tag{25}$$

The comparison was performed for $Re = 5 \times 10^4$. Figure 6 shows the comparison for triangular arrays. There is a large difference among the different correlations. The correlation by Ingesson and Hedberg gives much higher values than the data fit. Also the correlation by Zhukov *et al.* is high for $S/D < 0.2$, provided it has been applied correctly. The correlations by Rogers and Tahir and by Cheng and Todreas agree quite well for $S/D > 0.08$. The data fit (equation (19)) is in the middle of all the correlations. The picture is different for square arrays: all correlations and the data fit agree within a factor of about two (Fig. 7).

DEDUCTIONS FROM MACROSCOPIC FLOW PULSATIONS

Möller [61] showed from his measurements of the macroscopic flow pulsations that the mixing between subchannels is caused by the flow pulsations. From the power spectra for the velocity component parallel to the walls, Möller calculated the mixing velocity w^{M}_{eff} to be

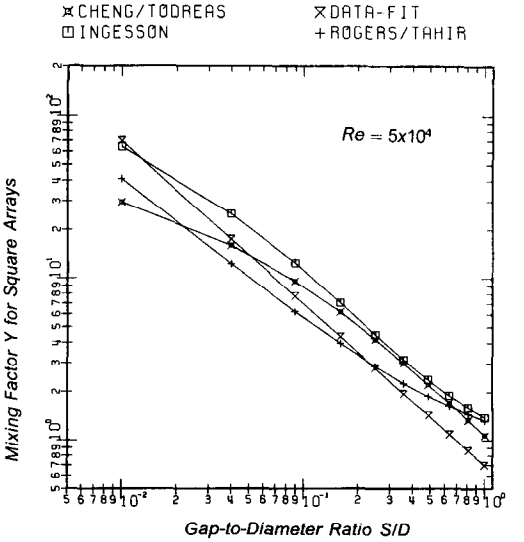

FIG. 7. Correlations for the mixing factor Y of rod bundles arranged in a square array.

$$w_{\text{eff}}^{\text{M}} = \sqrt{(\Phi_{ww}(f_{\text{peak}})B)} \tag{26}$$

where Φ_{ww} is the power spectral density in the gap centre at the peak frequency (Fig. 4) at which the flow pulsations occur and B the bandwidth of the digitalization ($B = 3.9063$ Hz). With this mixing velocity, he computed a mixing factor according to equation (17)

$$Y = \frac{w_{\text{eff}}^{\text{M}}\delta_{ij}}{\bar{\varepsilon}}. \tag{27}$$

Möller reported the following correlation for the mixing factor Y based on the data of his study

$$Y = 0.42\left(\frac{S}{D}\right)^{-1.547}. \tag{28}$$

The weakness of Möller's evaluation of the mixing velocity lies in the facts that (1) he uses the power spectral density of the velocity components parallel to the walls in the centre of the gap and (2) only the bandwidth of the peak frequency. The spectra reported by Möller [61, 62] clearly show that away from the centre of the gap the spectral density decreases both in the direction to the walls and in the direction on the subchannel symmetry line. Moreover, the peaks in the spectra extend over a certain frequency range (Fig. 4) and the peaks broaden at positions away from the centre of the gap. This means that the flow pulsations are not caused by large-scale eddies of one size at a certain frequency but by a spectrum of eddies of different sizes.

Therefore, Möller's experimental data have been recalculated. The peaks in the spectra of the velocity component parallel to the wall w' have been integrated over the half-width of the peak. The thus obtained effective mixing velocities were normalized to $Re = 5 \times 10^4$ assuming that w_{eff} is proportional to $Re^{0.9}$ in agreement with the dependence on the Reynolds number of most of the experimental mixing data. The data were correlated as a function of the normalized distance from the gap. The distance from the gap z ($z = 0$ at the gap) was made dimensionless by the centroid distance δ_{ij}.

The correlations of the data can be given as

$$w_{\text{eff}} = w_{\text{eff},z=0}\,10^{-0.4075(S/D)^{-0.44}(z/\delta_{ij})} \tag{29}$$

for the gap between the rods, and

$$w_{\text{eff}} = w_{\text{eff},z=0}\,10^{-0.78(S/D)^{-0.33}(z/\delta_{ij})} \tag{30}$$

for the gap between the rod and channel wall.

It was assumed that an effective mixing velocity can be calculated for $z/\delta_{ij} = 0.2$. This mixing velocity was multiplied by a factor of 0.85 to account for a profile of the mixing velocity, since all data were measured either at the centre of the gap or along the symmetry line. All data are listed in Tables 2 and 3 together with the mixing factors calculated according to equation (27).

Table 2. Mixing factors recalculated from Möller's data for gaps between the rods

Gap ratio S/D	Effective velocity w_{eff} (m s^{-1}) for $z/\delta_{ij} = 0.2$	Mixing factor Y
0.007	0.632	40.75
0.007	0.579	37.35
0.018	0.586	37.54
0.018	0.458	29.33
0.036	0.292	18.44
0.036	0.305	19.27
0.036	0.295	18.65
0.036	0.341	20.65
0.036	0.295	17.88
0.036	0.377	22.63
0.036	0.309	18.59
0.036	0.362	21.72
0.072	0.125	7.75
0.072	0.135	8.33
0.072	0.078	4.84
0.072	0.114	7.06
0.072	0.095	5.89
0.072	0.115	7.09
0.072	0.081	5.01
0.072	0.106	6.56
0.072	0.080	4.95
0.072	0.085	5.27
0.072	0.226	13.93
0.100	0.213	13.16
0.100	0.124	7.47
0.148	0.128	7.70
0.148	0.114	6.63
0.148	0.121	7.04
0.148	0.111	6.44
0.148	0.101	5.88
0.148	0.083	4.62
0.148	0.131	6.53
0.223	0.037	1.98

The mixing factors re-evaluated from Möller's study are plotted in Fig. 8 vs the relative gap width S/D.

A least square fit yields

$$Y = 0.812\left(\frac{S}{D}\right)^{-0.96} \tag{31}$$

which is in rather good agreement with the fit of all experimental mixing results, equation (19).

It can be concluded from the rather good agreement between the experimental mixing factors from the literature and the mixing factors evaluated from the macroscopic flow pulsations that the macroscopic flow pulsations are the reason for the relatively high mixing rates in rod bundles. It can further be concluded that secondary flows in subchannels of rod bundles do not contribute significantly to the mixing rates.

A comparison between the experimental mixing factors and the proposed simple correlation

Table 3. Mixing factors recalculated from Möller's data for gaps between rod and channel wall

Gap ratio S/D	Effective velocity w_{eff} (m s^{-1}) for $z/\delta_{ij} = 0.2$	Mixing factor Y
0.045	0.269	21.22
0.072	0.173	13.68
0.072	0.185	14.66
0.072	0.236	18.50
0.072	0.251	19.70
0.072	0.197	15.93
0.072	0.251	20.29
0.072	0.179	14.44
0.072	0.256	20.64
0.072	0.171	15.32
0.072	0.165	14.72
0.072	0.178	15.87
0.072	0.181	16.20
0.072	0.227	18.98
0.072	0.198	16.50
0.072	0.226	18.84
0.072	0.223	18.65
0.072	0.235	19.58
0.072	0.235	19.58
0.072	0.186	15.93
0.072	0.204	17.44
0.148	0.034	2.70
0.148	0.024	1.89
0.148	0.020	1.44
0.148	0.026	1.82
0.183	0.033	2.73
0.225	0.015	1.07

$$Y = \frac{0.7}{S/D} \tag{19}$$

is shown in Figs. 9 and 10 for triangular and square arrays, respectively. Whereas most experimental data are lower than equation (19) for triangular arrays, the correlation is in rather good agreement with the experimental data for square arrays. For triangular arrays, the scatter of the data is much higher than for square arrays. It cannot be decided if the shape of the gap affects mixing. More reliable data are needed. It should also be interesting to obtain results on the flow pulsations between subchannels of rod bundles in triangular arrays.

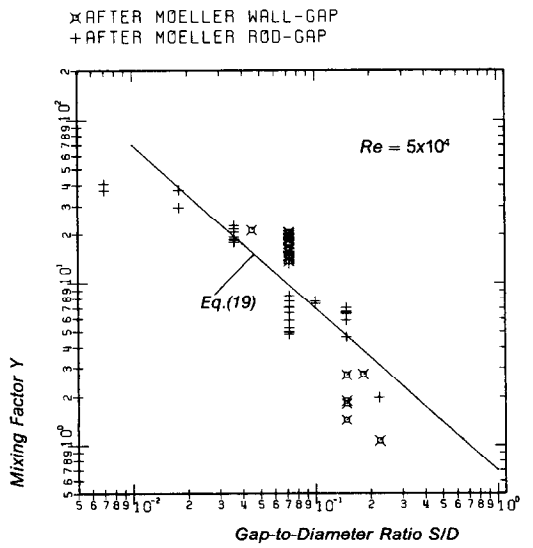

FIG. 8. Mixing factors Y calculated from Möller's power spectra.

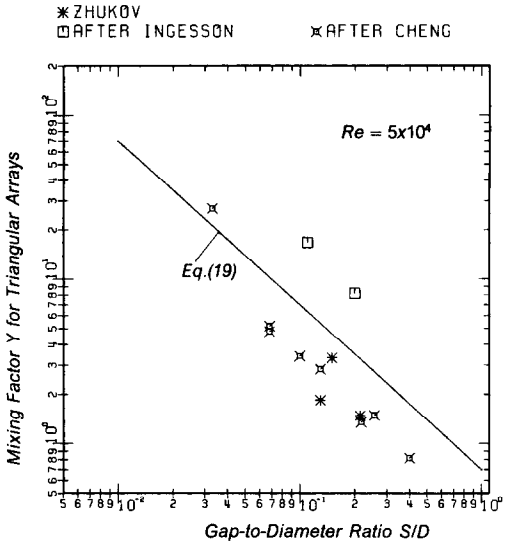

FIG. 9. Comparison between the experimental mixing factors Y in the gaps of rod bundles arranged in a triangular array and equation (19).

CONCLUSIONS

The experimental data on natural mixing between subchannels of rod bundles by turbulent interchange have been reviewed. In the light of the present knowledge on the structure of turbulence in subchannels of rod bundles it can be concluded that the almost

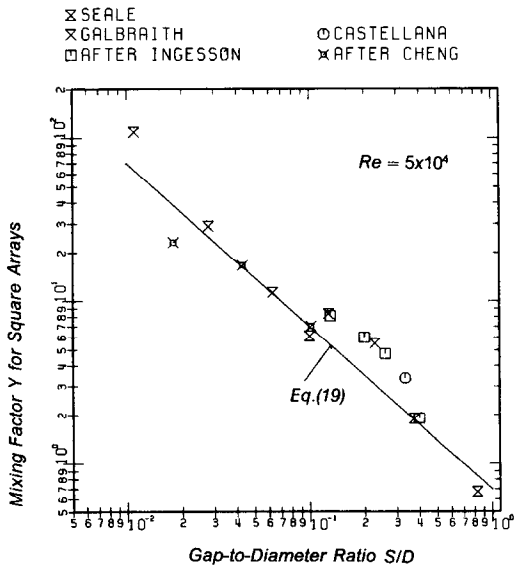

FIG. 10. Comparison between the experimental mixing factors Y in the gaps of rod bundles arranged in a square array and equation (19).

periodical flow pulsations between subchannels are the main reason for the natural mixing between subchannels of rod bundles. The secondary flow motion in subchannels does not contribute significantly to the mixing process.

Mixing factors deduced from spectra measurements by Möller are in rather good agreement with the experimental data on mixing reported in the literature. A simple correlation of the mixing factor was developed which may be used for any gap geometry as a good approximation.

Acknowledgement—The author wishes to thank Dr Walter Väth, KfK–INR, for many fruitful discussions on the evaluation of the effective mixing velocity from the power spectra and Prof. Neil E. Todreas, MIT, for his useful comments to improve the manuscript.

REFERENCES

1. N. E. Todreas and L. W. Wilson, Coolant mixing in sodium cooled fast reactor fuel bundles, WASH-1096 (April 1968).
2. J. T. Rogers and N. E. Todreas, *Coolant Interchannel Mixing in Reactor Fuel Rod Bundles Single-phase Coolants, Heat Transfer in Rod Bundles* (Edited by V. E. Schrock). ASME, New York (December 1968).
3. D. E. Coates, Interchannel mixing and cooling temperature distribution in seven and nineteen element fuel bundles, X07-10001R, Canadian General Electric Company Ltd. (1960).
4. C. B. Moyer, Coolant mixing in multirod fuel bundles, Risö Report No. 125, July 1964 (Issued 1966).
5. D. S. Rowe and C. W. Angle, Cross-flow mixing between parallel flow channels during boiling (Part II), measurement of flow and enthalpy in two parallel channels, BNWL-371 Pt. 2, Battelle Northwest Laboratories (1967).
6. A. C. Rapier, Turbulent mixing in a fluid flowing in a passage of constant cross-section, TRG-Report-1417(W), UKAEA (1967).
7. J. T. Rogers and W. R. Tarasuk, A generalized correlation for natural turbulent mixing of coolant in fuel bundles, *Trans. ANS* **11**(1), 346 (1968).
8. V. R. Skinner, A. R. Freeman and H. G. Lyall, Gas mixing in rod clusters, *Int. J. Heat Mass Transfer* **12**, 265–278 (1969).
9. L. Ingesson and B. Kjellström, On gas mixing in rod bundles, *Int. J. Heat Mass Transfer* **13**, 429–431 (1970).
10. L. Ingesson and S. Hedberg, Heat transfer between subchannels in a rod bundle, *Heat Transfer 1970*, Paris, Vol. III, FC.7.11. Elsevier, Amsterdam (1970).
11. T. van der Ros and M. Bogaardt, Mass and heat exchange between adjacent channels in liquid-cooled rod bundles, *Nucl. Engng Des.* **12**, 259–268 (1970).
12. G. Hofmann, Qualitative investigation of local heat transfer coefficients in a 7-rod bundle, Report No. 13. Institut für Reaktorbauelemente, KfK Karlsruhe, F.R.G. (June 1964) (in German—unpublished).
13. K. P. Galbraith and J. G. Knudsen, Turbulent mixing between adjacent channels for single-phase flow in a simulated rod bundle, 12th Natn. Heat Transfer Conf., Tulsa, Oklahoma, A.I.Ch.E. Symp. Series, pp. 90–100 (1971).
14. K. Singh and C. C. St. Pierre, Single phase turbulent mixing in simulated rod bundle geometries, *Trans. CSME* **1**(2), 73–80 (1972).
15. W. Eifler und R. Nijsing, Turbulenter Reibungsbeiwert und Mischungsbeiwert für den Impulsaustausch zwischen Unterkanälen—typische Beispiele für nicht-universelle Gesetzmäßigkeiten, Reaktortagung 1972, pp. 7–10, Deutsches Atomforum e.V., Bonn (1972).
16. D. S. Rowe, Measurement of turbulent velocity, intensity and scale in rod bundle flow channels, BNWL-1736, Battelle Pacific Northwest Laboratories, Richland, Washington (1973).
17. D. S. Rowe, B. M. Johnson and J. G. Knudsen, Implications concerning rod bundle crossflow mixing based on measurements of turbulent flow structure, *Int. J. Heat Mass Transfer* **14**, 407–419 (1974).
18. J. T. Rogers and A. E. E. Tahir, Turbulent interchange mixing in rod bundles and the role of secondary flows, ASME Paper 75-HT-31 (1975).
19. W. J. Seale, The effect of subchannel shape on heat transfer in rod bundles with axial flow, *Int. J. Heat Mass Transfer* **24**, 768–770 (1981).
20. B. Kjellström, Studies of turbulent flow parallel to a rod bundle of triangular array, AE-487, Aktiebolaget Atomenergie, Studsvik (1974).
21. G. Markoczy and M. Huggenberger, Verification of subchannel analysis computer codes by a full-scale experiment, *Trans. 1st Conf. European Nuclear Society*, Paris, pp. 758–761 (1975).
22. A. Martelli, Thermo-fluiddynamic analysis of gas cooled fuel element bundles, Dr.-Ing. Dissertation, University Karlsruhe (1977) (in German).
23. S. Cevolani, Thermo- and fluiddynamic analysis of gas cooled fuel element bundles taking into account thermal radiation and thermal conduction, Dr.-Ing. Dissertation, University Karlsruhe (1981) (in German).
24. J. D. Hooper and K. Rehme, The structure of single-phase turbulent flows through closely spaced rod arrays, KfK 3467, Kernforschungszentrum Karlsruhe, F.R.G. (1983).
25. J. D. Hooper and K. Rehme, Large-scale structural effects in developed turbulent flow through closely-spaced rod arrays, *J. Fluid Mech.* **145**, 305–337 (1984).
26. S.-K. Cheng and N. E. Todreas, Constitutive correlations for wire-wrapped subchannel analysis under forced and mixed convection conditions, Report No. DOE/ET/37240-108 TR, MIT, Cambridge, Massachusetts (1984).
27. S.-K. Cheng and N. E. Todreas, Hydrodynamic models and correlations for bare and wire-wrapped hexagonal rod bundles—bundle friction factors, subchannel friction factors and mixing parameters, *Nucl. Engng Des.* **92**, 227–251 (1986).
28. A. V. Zhukov, A. P. Sorokin and N. M. Matyukhin, Megkanalnyi obmen v TVS bystrych reaktorov, Energoatomisdat, *Physika i Technika jadernych reaktorov, Moskva, Energoatomisdat, Vypusk* 38 (1989) (Interchannel exchange in heated rod bundles of fast breeder reactors, *Series Physics and Technique of Nuclear Reactors* 38).
29. Ch. Hall and P.-J. Svenningson, Secondary flow velocities in a rod bundle of triangular array, AE-RL-1326, Aktiebolaget Atomenergi, Studsvik (1971).
30. A. C. Trupp and R. S. Azad, Turbulent flow in triangular rod bundles, *Nucl. Engng Des.* **32**, 47–84 (1975).
31. P. Carajilescov and N. E. Todreas, Experimental and analytical study of axial turbulent flows in an interior subchannel of a bare rod bundle, COO-2245-19 TR, MIT, Cambridge, Massachusetts (1975); cf. *ASME J. Heat Transfer* **98**, 262–268 (1976).
32. J. Nikuradse, Untersuchungen über turbulente Strömungen in nicht kreisförmigen Rohren, *Ing.-Arch.* **1**, 306–332 (1930).
33. L. C. Hoagland, Fully developed turbulent flow in straight rectangular ducts, Ph.D. Thesis, MIT, Cambridge, Massachusetts, OOR-1935.2 (1960).
34. E. Brundrett and W. D. Baines, The production and diffusion of vorticity in duct flow, *J. Fluid Mech.* **19**, 375–394 (1964).

35. F. B. Gessner and J. B. Jones, On some aspects of fully-developed turbulent flow in rectangular channels, *J. Fluid Mech.* **23,** 689–713 (1965).
36. B. E. Launder and W. M. Ying, Secondary flows in ducts of square cross-section, *J. Fluid Mech.* **54,** 289–295 (1972).
37. A. Melling and J. H. Whitelaw, Turbulent flow in a rectangular duct, *J. Fluid Mech.* **78,** 289–315 (1976).
38. A. M. M. Aly, A. C. Trupp and A. D. Gerrard, Measurements and prediction of fully developed turbulent flow in an equilateral triangular duct, *J. Fluid Mech.* **85,** 57–83 (1978).
39. M. M. A. Khalifa and A. C. Trupp, Measurements of fully developed turbulent flow in a trapezoidal duct, *Exp. Fluids* **6,** 344–352 (1988).
40. W. J. Seale, Measurements and predictions of fully developed turbulent flow in a simulated rod bundle, *J. Fluid Mech.* **123,** 399–423 (1982).
41. K. Rehme, Measurements of the velocity, turbulence and wall shear stress distributions in a corner channel of a rod bundle, KfK 2512, Kernforschungszentrum Karlsruhe (1977) (in German).
42. K. Rehme, Anisotropic eddy viscosities in the turbulent flow through a rod bundle, Symp. on Turbulent Shear Flows, University Park, Pennsylvania, 18–20 April 1977, Paper 8F (1977).
43. W. J. Seale, Turbulent diffusion of heat between connected flow passages, Part 1: outline of problem and experimental investigation, *Nucl. Engng Des.* **54,** 183–195 (1979).
44. W. J. Seale, Turbulent diffusion of heat between connected flow passages, Part 2: predictions using the "k–ε" turbulence model, *Nucl. Engng Des.* **54,** 197–209 (1979).
45. V. Vonka, Measurement of secondary flow vortices in a rod bundle, *Nucl. Engng Des.* **106,** 191–207 (1988).
46. N. Neelen, Modellierung des Impulstransports achsparalleler turbulenter Strömungen, Dr.-Ing. Dissertation, TU Braunschweig (1987).
47. C. Monir, Bedeutung des Sekundärströmungsterms bei der Berechnung turbulenter Strömungen durch enge hexagonale Stabgitter mit dem Modell VELASCO-TUBS, Bericht K8724, Institut für Raumflug- und Reaktortechnik, TU Braunschweig (1987).
48. J. G. Bartzis and N. E. Todreas, Turbulence modeling of axial flow in a bare rod bundle, *J. Heat Transfer* **101,** 628–634 (1979).
49. K. Rehme, Experimental investigation of the turbulent flow through a wall subchannel of a rod bundle, KfK 2441, Kernforschungszentrum Karlsruhe (1977).
50. K. Rehme, The structure of turbulent flow through rod bundles, *Nucl. Engng Des.* **99,** 141–154 (1987).
51. K. Rehme, The structure of turbulence in wall subchannels of rod bundles, *Atomkernenergie-Kerntechnik* **49,** 145–150 (1987).
52. K. Rehme, Geschwindigkeits- und Turbulenzverteilungen in Wandkanälen von Stabbündeln mit einem Gitterabstandshalter, KfK 4094, Kernforschungszentrum Karlsruhe (1986).
53. S. R. Wu and K. Rehme, An experimental investigation on turbulent flow through symmetric wall subchannels of two rod bundles, *Nucl. Technol.* **89,** 103–115 (1990).
54. K. Rehme, On the development of turbulent flow in wall subchannels of rod bundles, *Nucl. Technol.* **77,** 331–342 (1987).
55. K. Rehme, Experimental observations of turbulent flow through subchannels of rod bundles, *Exp. Thermal Fluid Sci.* **2,** 341–349 (1989).
56. C. J. Lawn, Application of the turbulence energy equation to fully developed flow in simple ducts: figures and figure captions, Report RD/B/R 1575 (C), Central Electricity Generating Board, Berkeley, U.K. (1970).
57. A. E. E. Tahir and J. T. Rogers, Turbulent flow structure in a closely-spaced triangular-array rod bundle, *Heat Transfer 1986, Proc. 8th Heat Transfer Conf.*, San Francisco, California, 17–22 August 1986 (Edited by C. L. Tien *et al.*), Vol. 3, pp. 1035–1040. Hemisphere, Washington, DC (1986).
58. J. Hejna and F. Mantlik, The structure of turbulent flow in finite rod bundles, *1st World Conf. on Experimental Heat Transfer, Fluid Mechanics, and Thermodynamics*, Dubrovnik (Edited by R. K. Shah, E. N. Ganic and K. T. Yang), pp. 1712–1719. Elsevier, Amsterdam (1988).
59. J. Hejna and L. Vosáhlo, Personal communication (1984).
60. H. Reichardt, Vollständige Darstellung der turbulenten Geschwindigkeitsverteilung in glatten Leitungen, *Z. Angew. Math. Mech.* **31,** 208–219 (1951).
61. S. V. Möller, Experimental study of the phenomena of turbulent flow in the narrow gaps between subchannels of rod bundles, KfK 4501, Kernforschungszentrum Karlsruhe, F.R.G. (1989) (in German).
62. S. V. Möller, On phenomena of turbulent flow through rod bundles, *NURETH-4, Proc. Fourth Int. Top. Mtg on Nucl. Reactor Thermal-Hydraulics*, Karlsruhe, F.R.G., October 1989 (Edited by U. Müller, K. Rehme and K. Rust), Vol. 2, pp. 1287–1293 (1989), cf. *Exp. Thermal Fluid Sci.* **4**(1), 25–35 (1991).
63. S. Horanyi, L. Krebs and G. Weinkötz, Measurement and analysis of temperature fluctuations in the sodium-cooled 4-rod bundle TEGENA, *NURETH-4, Proc. Fourth Int. Top. Mtg on Nucl. Reactor Thermal-Hydraulics*, Karlsruhe, F.R.G., October 1989 (Edited by U. Müller, K. Rehme and K. Rust), Vol. 2, pp. 1279–1286 (1989).
64. C. Chiu, N. Todreas and R. Morris, Experimental techniques for liquid metal cooled fast breeder reactor fuel assembly thermal/hydraulic tests, *Nucl. Engng Des.* **62,** 253–270 (1980).
65. J. W. Elder, The dispersion of marked fluid in turbulent shear flow, *J. Fluid Mech.* **5,** 544–560 (1959).
66. W. H. Bell and B. W. LeTourneau, Experimental measurements of mixing in parallel flow rod bundles, WAPD-TH-381, Westinghouse Electric Corp., Pittsburgh (1958).
67. W. M. Biggs and J. H. Rust, A study of interchannel mixing employing activation analysis, *Trans. ANS* **10**(2), 656–657 (1967).
68. A. A. Bishop, P. A. Nelson and L. S. Tong, Coolant mixing in a nineteen-rod fuel assembly, *Trans. ANS* **4**(1), 43–44 (1961).
69. G. J. Clarke, Mixing studies of types C19A14B, C19A14C, and C19X8D fuel bundles, TDVI-19 (1961).
70. R. D. Collins and J. France, Mixing of coolant in channels between close-packed fuel elements, IGR-TN/CA-847, UKAEA (1958).
71. L. Ingesson, S. Rolandsson and S. Hedberg, Internal Report RTL-990, AB Atomenergi, Studsvik (1968).
72. J.-E. Jonsson, Internal Report RPL-107, AB Atomenergi, Studsvik (1962).
73. J.-E. Jonsson, Internal Report RPL-608, AB Atomenergi, Studsvik (1962).
74. H. Knaab and H. Stehle, Bestrahlung eines MZFR-Testbrennelementes im NRX-Reaktor, *Nukleonik* **7**(5), 209–217 (1965).
75. I. Multer, Internal Report RMB-352, AB Atomenergi, Studsvik (1963).
76. P. A. Nelson, A. A. Bishop and L. S. Tong, Mixing in flow parallel to rod bundles having a square lattice, WCAP-1607, Westinghouse Electric Corp., Pittsburgh (1960).
77. J. T. Rogers and W. R. Tarasuk, Inter-sub-channel coolant mixing in close-packed reactor fuel bundles, Part I—natural mixing, R64CAP29-I, Canadian General Electric (1966).
78. E. D. Waters, Fluid mixing experiments with a wire-

wrapped 7-rod bundle fuel assembly, HW-70178 REV, Hanford Atomic Products Operation, Richland (1963).
79. K. Petrunik, Turbulent mixing measurements for single phase air, single phase water, and two phase air–water flows in adjacent rectangular subchannels, M.A.Sc. Thesis, University of Windsor, Ontario (1968).
80. B. Kjellström, Transport process in turbulent channel flow, Final Report AE-RL-1344, Aktiebolaget Atomenergi, Studsvik (1971).
81. M. Roidt, M. J. Pechersky, R. A. Markley and B. J. Vegter, Determination of turbulent exchange coefficients in a rod bundle, *J. Heat Transfer* 172–177 (1974).
82. F. B. Walton, Turbulent mixing measurements for single phase air–water flows in adjacent triangular subchannels, M.A.Sc. Thesis, University of Windsor, Ontario (1969).
83. J. Kelly and N. E. Todreas, Turbulent interchange in triangular array bare rod bundles, COO-2245-45TR, MIT (1977), cf. *Proc. Sixth Int Heat Transfer Conf.*, Toronto, Canada, 7–11 August, Vol. 5, pp. 11–16 (1978).
84. F. S. Castellana, W. T. Adams and J. E. Casterline, Single-phase subchannel mixing in a simulated nuclear fuel assembly, *Nucl. Engng Des.* **26**, 242–249 (1974).
85. A. V. Zhukov, N. A. Kotovskii, L. K. Kudryavtseva, N. M. Matyukhin, E. Ya. Sviridenko, A. P. Sorokin, P. A. Ushakov and Yu. S. Yur'ev, Comecon-Symposium "Teplofizika i gidrodinamika aktivnoi zony i parogeneratorov dlya bystrykh reaktorov" Marianské Lazne, CSSR, 4.-7.4. 1978, CKAE, Prag, Vol. 1, paper ML78/09, pp. 114–127 (1978) (in Russian); German transl. KfK-tr-657, Kernforschungszentrum Karlsruhe, F.R.G. (1980).

APPENDIX

The different definitions for mixing rates between subchannels of rod bundles are converted into a mixing factor introduced by Ingesson and Hedberg [10] (equation (17))

$$Y = \frac{w_{\text{eff}}\delta_{ij}}{\bar{\varepsilon}}.$$

(1) Mixing number w'_{ij}/μ [18]

$$Y = \frac{w'_{ij}\delta_{ij}}{\rho S\bar{\varepsilon}}$$

and with equation (16)

$$Y = \left(\frac{w'_{ij}}{\mu}\right)\frac{\delta_{ij}}{S}\frac{20}{Re\sqrt{\left(\frac{\lambda_T}{8}\right)}}$$

$$\delta_{ij} = P \quad \text{for square arrays}$$

$$\delta_{ij} = \frac{P}{\sqrt{3}} \quad \text{for triangular arrays}$$

$$\lambda_T = 0.18\,Re^{-0.2}, \quad Re\sqrt{\left(\frac{\lambda_T}{8}\right)} = 0.15\,Re^{0.9}.$$

(2) Mixing rate per unit length μ_T [28]

$$\mu_T = \frac{w'_{ij}}{m_i}, \quad Y = \frac{w'_{ij}\delta_{ij}}{\rho S\bar{\varepsilon}}, \quad Y = \mu_T\frac{m_i\delta_{ij}}{\rho S\bar{\varepsilon}}$$

$$\frac{m_i}{\rho} = \nu\frac{Re_iP_i}{4}, \quad Y = \mu_T\frac{\delta_{ij}}{S}\frac{5P_i}{\sqrt{\left(\frac{\lambda_T}{8}\right)}}$$

$$P_i = \frac{D\pi}{2} \quad \text{for triangular arrays}$$

$$P_i = D\pi \quad \text{for square arrays.}$$

(3) Gap Stanton number $\varepsilon^*_{\eta T}$ [26]

$$\varepsilon^*_{\eta T} = St_g = \frac{w_{\text{eff}}}{u_{\text{av},i}}, \quad Y = \varepsilon^*_{\eta T}\frac{u_{\text{av},i}\delta_{ij}}{\bar{\varepsilon}}$$

$$Y = \varepsilon^*_{\eta T}\frac{20u_{\text{av},i}\delta_{ij}}{\nu\frac{u_{\text{av},i}D_h}{\nu}\sqrt{\left(\frac{\lambda_T}{8}\right)}}, \quad Y = \varepsilon^*_{\eta T}\frac{\delta_{ij}}{D_h}\frac{20}{\sqrt{\left(\frac{\lambda_T}{8}\right)}}$$

$$\frac{\delta_{ij}}{D_h} = \frac{P/D}{\frac{6}{\pi}\left(\frac{P}{D}\right)^2 - \sqrt{3}} \quad \text{for triangular arrays}$$

$$\frac{\delta_{ij}}{D_h} = \frac{P/D}{\frac{4}{\pi}\left(\frac{P}{D}\right)^2 - 1} \quad \text{for square arrays.}$$

The non-dimensional mixing factor β [78] is the gap Stanton number.

LA STRUCTURE DE LA TURBULENCE DANS DES GRAPPES DE CYLINDRES ET LES IMPLICATIONS SUR LE MELANGE NATUREL ENTRE LES SOUS-CANAUX

Résumé—On passe en revue les données expérimentales sur le mélange naturel entre les sous-canaux des grappes de cylindres par interchange turbulent. On discute les caractères principaux de la structure de la turbulence dans les sous-canaux. On conclut que des pulsations cycliques et souvent périodiques de l'écoulement à travers les espaces libres de la grappe sont la raison de flux de mélange observés lesquels sont relativement indépendants de la largeur de l'espace entre tubes. Une corrélation simple d'un facteur de mélange est donnée et elle peut être utilisée comme une bonne approximation pour une géométrie quelconque.

DIE TURBULENZSTRUKTUR IN STABBÜNDELN UND DIE VERBINDUNG ZUR NATÜRLICHEN MISCHUNG ZWISCHEN DEN UNTERKANÄLEN

Zusammenfassung—Die experimentellen Ergebnisse zur natürlichen Mischung zwischen Unterkanälen von Stabbündeln durch turbulenten Austausch werden zusammengefaßt. Die Hauptmerkmale der Turbulenzstruktur in Unterkanälen von Stabbündeln werden dargestellt. Es kann geschlossen werden, daß zyklische und fast periodische Strömungspulsationen die Ursache für die beobachteten Mischraten durch die Spalte sind, die relativ unabhängig von der Spaltweite sind. Eine einfache Beziehung wird für den Mischungsfaktor entwickelt, die mit guter Näherung für jede Spaltgeometrie verwendet werden kann.

СТРУКТУРА ТУРБУЛЕНТНОСТИ В СТЕРЖНЕВЫХ ПУЧКАХ И ЕЕ ВЛИЯНИЕ НА ЕСТЕСТВЕННОЕ СМЕШЕНИЕ МЕЖДУ ОБРАЗОВАННЫМИ ИМИ КАНАЛАМИ

Аннотация—Приводятся экспериментальные данные по естественному смешению между каналами стержневых пучков, происходящему за счет турбулентного обмена. Обсуждаются основные особенности структуры турбулентности в таких каналах и делается вывод, что циклические и почти периодические колебания потока в зазорах между пучками стержней обуславливают наблюдаемые скорости смешения, которые не зависят от ширины зазора. Разработано простое обобщающее соотношение для описания коэффициента смешения, которое может использоваться в качестве хорошего приближения при любой геометрии зазора.